The Meteoritical Society

Meteoritics & Planetary Science 48, Nr 4, 686–699 (2013)
doi: 10.1111/maps.12093

Refractory metal nuggets within presolar graphite: First condensates from a circumstellar environment

T. K. CROAT[1*], T. BERG[2,3], T. BERNATOWICZ[1], E. GROOPMAN[1], and M. JADHAV[4]

[1]Laboratory for Space Sciences, Physics Department, Washington University, CB1105 1 Brookings Drive, Saint Louis, Missouri 63130, USA
[2]Institut fur Physik, Johannes Gutenberg-Universität, Staudingerweg 7, Mainz D-55128, Germany
[3]Max-Planck-Institut für Chemie, Joh.-Joachim-Becher-Weg 27, Mainz D-55128, Germany
[4]Hawai'i Institute of Geophysics and Planetology, University of Hawai'i at Manoa, Honolulu, Hawai'i 96822, USA
[*]Corresponding author. E-mail: tkc@wustl.edu

(Received 09 December 2011; revision accepted 14 January 2013)

Abstract–Transmission electron microscope (TEM) investigations have revealed Os, Ru, Mo-rich refractory metal nuggets within four different presolar graphites, from both the high-density (HD) Murchison (MUR) and low-density (LD) Orgueil (ORG) fractions. Microstructural and chemical data suggest that these are direct condensates from the gas, rather than forming later by exsolution. The presolar refractory metal nugget (pRMN) compositions are variable (e.g., from $8 <$ Os atom% < 77), but follow the same chemical fractionation trends as isolated refractory metal nuggets (mRMNs) previously found in meteorites (Berg et al. 2009). From these compositions one can infer a temperature of last equilibration with the gas of 1405–1810 K (e.g., Berg et al. [2009] at approximately 100 dyne cm^{-2} pressure), which implies that the host graphites form over roughly the same range (in agreement with predictions) and that the pRMNs are chemically isolated from the gas when captured by graphite. Further, the pRMN compositions give evidence that HD graphites form at a higher T than LD ones. Chemical and phase similarities with the isolated mRMNs suggest that the mRMNs also condense directly from a gas, although from the early solar nebula rather than a presolar environment. Although the pRMNs themselves are too small for detection of isotopic anomalies, NanoSIMS isotopic measurements of their host graphites confirm a presolar origin for the assemblages. The two pRMN-containing LD graphites show evidence of a supernova (SN) origin, whereas the stellar origins of the pRMNs in HD graphite are unclear, because only less-diagnostic ^{12}C enrichments are detectable (as is commonly true for HD graphites).

INTRODUCTION

A peculiar class of refractory metal grains heavily enriched in Pt group elements was first found associated with CAIs in meteorites (Palme and Wlotzka 1976; Wark and Lovering 1976). These grains are often enriched in Os, W, Ru, and other refractory elements at several thousand times the CI values, but can show significant compositional variations sometimes in the same refractory inclusion. Further studies (El Goresy et al. 1978) showed that these grains had two distinct modes of occurrence, sometimes being found as larger isolated refractory metal nuggets but in other cases were found within complex opaque assemblages in close association with Fe-Ni metal, sulfide, phosphate, silicate, and oxide phases (referred to as Fremdlinge). Models showed that refractory metal grains with a composition similar to those observed are predicted to condense from solar gas at high temperature, suggesting these grains were solid condensates either from the solar nebula or perhaps presolar grains from other stellar environments (Grossman [1980] and refs therein). The complex Fremdlinge assemblages then could form when the already-condensed refractory metal nuggets and

iron-nickel metal grains were mixed with proto-CAI material during brief high temperature events, dispersing the metal grains in partially or completely melted CAI material followed by rapid cooling (MacPherson et al. 1988). However, solidification experiments on Ni-Ru-Fe-O alloys suggested an alternative scenario wherein Fremdlinge form from homogeneous molten drops via exsolution (Blum et al. 1988). Immiscible regions in the Ni-Ru-Fe-O phase diagram cause partitioning into more refractory Ru-rich metal and iron-nickel metal, followed by oxidation and sulfidization reactions, resulting in a solidification microstructure quite similar to that of Fremdlinge. The isolated nuggets are not addressed by this model, but it is suggested that these could be precipitated directly from CAI silicate liquid or are remnants of digested opaque assemblages.

Isotopic measurements of Mg, Fe, Mo, Ru, and W in Fremdlinge from Allende CAIs yielded solar isotopic ratios (Hutcheon et al. 1987), suggesting an origin in the solar nebula rather than a presolar grain origin. Isotopic measurements on the smaller isolated refractory metal nuggets are more limited (one for Ru by Hutcheon et al. [1987] and another for Os by Berg et al. [2009]), but again no isotopic anomalies were found. Based on these isotopic results as well as the phase and chemical compositions of hundreds of isolated refractory metal nuggets in the meteorite (hereafter referred to as mRMNs), Berg et al. (2009) argue that these grains are the first condensates from the solar nebula. The mRMNs have appreciable W and Mo content, which is consistent with condensation under reducing conditions and inconsistent with other scenarios where the RMNs would lose W and Mo when heated under oxidizing conditions. The chemical compositions are quite variable, but such variations are consistent with elemental fractionation that depends on the temperature of last equilibration with the gas. If these mRMNs are in fact the preserved first condensates from the solar system, then one could use their properties to infer the thermal history of the gas from which they condensed.

If mRMNs are high temperature solid condensates from reducing environments, one might expect them also to be found preserved in presolar graphites. Included grains of refractory phases are commonly found within presolar graphites, including ubiquitous titanium carbides (TiCs) but also silicon carbide, iron carbide, iron-nickel metal, and even oxides such as rutile and spinel (Bernatowicz et al. 1996, 2006; Croat et al. 2003, 2010a). The chemical and microstructural diversity of internal TiCs found within the same graphite suggest that they condensed independently from the gas and then were captured and entrained during the graphite's growth (Croat et al. 2003). Such observations, along with the very low concentrations of all elements but C in the graphites, rule out exsolution as a viable formation scenario. Thus, the types of phases present within graphite and their microstructures allow the condensation sequence to be inferred, which in turn can be used to place constraints on the temperatures and pressures in the gas from which the grains condensed (e.g., Bernatowicz et al. 1996; Croat et al. 2003). The chemical, microstructural, and isotopic properties of the various internal grains yield further information about their formation environment. The isotopic signatures from various presolar graphites show that the presolar graphite population contains stardust both from massive stars such as Type II supernova and from asymptotic giant branch (AGB) carbon stars. In many cases the internal grains themselves have shown large isotopic anomalies, such as inferred ^{44}Ti excesses in low-density SN carbides (Stadermann et al. 2005) and ^{29,30}Si enrichments in unusual SiCs within high-density graphite (Croat et al. 2010a), both of which indicate a massive star origin. Other carbides within high-density graphites show strong *s*-process element enrichments indicative of an AGB origin.

Here, we report the discovery of four different refractory metal nuggets found inside ultramicrotomed sections of presolar graphite grains, two from the Murchison KFC1 high-density fraction (Amari et al. 1994) and two from the Orgueil OR1d low-density fraction (Jadhav et al. 2006; Groopman et al. 2012). Hereafter, these presolar RMNs will be referred to as pRMNs so as to distinguish them from the mRMNs discussed previously. While the internal pRMNs themselves are too small for independent isotopic measurement, the host graphites are clearly presolar grains. That the pRMNs are found inside of presolar graphites demonstrates that they are primary condensates that form directly from the gas in stellar outflows, as has been conclusively shown for other types of grains found within presolar graphites (e.g., Croat et al. 2003). Detailed studies of the pRMN compositions and crystal structures show considerable similarities with the larger mRMNs found within meteorite residues (Berg et al. 2009), although certain pRMNs are more refractory. While these features certainly do not imply that the isolated mRMN nuggets are presolar grains, the similarities in structure and composition do provide supporting evidence that the mRMNs may be direct solid condensates from the gas phase in the solar nebula (Berg et al. 2009).

SAMPLES AND EXPERIMENTAL METHODS

Two of the four pRMN-containing graphites (henceforth referred to as ORG1 and ORG2) originated

from the OR1d low-density (LD) size separate (1.75–1.92 g cm^{-3}; >1 μm) from the Orgueil (ORG) meteorite (Jadhav et al. 2006). In this separate, graphites were isolated from the ORG matrix material using techniques developed by Amari et al. (1994). Subsequent NanoSIMS measurements of the ORG1 graphite (8 μm diameter) were made of C, N, O, Al-Mg, Si, Ca, and Ti isotopes, which revealed that this grain was from the ^{13}C-rich graphite group. Further details on the multielement isotopic measurements of the bulk ORG1 graphite are available in Jadhav et al. (Forthcoming) (wherein ORG1 is named OR1d3m-7). NanoSIMS measurements of C, N, O, Al-Mg, and Si were made on the ORG2 graphite (approximately 5 μm diameter) and further isotopic data are available in Groopman et al. (2012) (wherein the graphite is named OR1d6m13). Since most of these relatively large grains were not consumed during NanoSIMS analyses, they were selected for coordinated TEM studies. The two ORG graphites were picked up from the NanoSIMS mount using a W needle attached to an Eppendorf Patchman NP2 micromanipulator and placed in gelatin or polyethylene BEEM® capsules along with carbon fibers to aid in locating the grains. The capsules were slowly filled with LR White hard resin and cured at 70 °C for 1 day in a vacuum furnace. The resin blocks containing the graphites were then sliced with a diamond-knife ultramicrotome into approximately 70 nm sections, which were then deposited on holey-carbon-coated copper TEM grids for ORG1 and SiO-coated copper TEM grids for ORG2. Sixteen cross sections of ORG1 (aka OR1d3m-7) and nine cross sections of ORG2 (aka OR1d6m13) were studied in TEM, and further details on this procedure are available in Croat et al. (2003).

Two of the four pRMNs were found within high-density (HD) graphites from the Murchison (MUR) KFC1 density and size separate (2.15–2.20 g cm^{-3}, >1 μm; Amari et al. 1994). Unlike the above Orgueil graphites, these grains were not individually picked and ultramicrotomed but rather were ultramicrotomed en masse. A droplet from this separate containing many MUR graphites (estimated to contain approximately 750 unique graphites) was deposited from suspension into a gelatin cylinder atop a glass slide, the entire deposit was embedded in resin, and then was sliced via ultramicrotomy into $\leq$100 nm thick sections (details in Bernatowicz et al. 1996). The stellar origins and morphologies of the same MUR KFC1 graphite population have been previously published (Croat et al. 2008), as have reports of a new type of massive star condensate, namely the unusual SiCs with heavy $^{29,30}Si$ anomalies found within graphites (Croat et al. 2010a). For the MUR graphites, all TEM analyses were completed prior to any isotopic measurements whereas for the ORG graphites ultramicrotomy and TEM were done after the NanoSIMS measurements. pRMNs were found in only 0.3% of high-density graphites (2 of approximately 750), but since only 10–20% of the graphite's volume is available for TEM analyses, the fraction that contain pRMNs could be higher (up to approximately 3%). The pRMNs are approximately 40× less common than the ubiquitous TiC internal grains in the same graphite population. pRMNs are also uncommon in low-density graphites, with only two pRMN yet found among approximately 25 LD graphites from Orgueil and Murchison studied in the TEM.

The pRMN-containing graphite cross sections were studied using a JEOL 2000FX TEM equipped with a NORAN ultra-thin window energy dispersive X-ray spectrometer (EDXS) and with a JEOL 2100 TEM. Quantitative EDXS analysis was performed on all internal grains using k-factors derived from geological standards of known composition (ilmenite USNM 96189, chromite USNM 117075, basaltic glass USNM 113498) and numerous stoichiometric oxides (lead titanate, lead zirconate, lead molybdate, calcium vanadate, calcium titanate, calcium phosphate, etc.) using the Cliff-Lorimer technique. No standards were available for Os, W, Ir, and Ru so in these cases k-factors suitable to the instrument were estimated based on the NORAN-provided standard values. Derived k-factors for elements with $Z > 11$ with respect to Ti (directly or indirectly) typically showed 3–10% variations (standard deviation). When an element of interest was not detected in a given pRMN, an upper limit was placed on its concentration using a 2σ above background level. Overlap of elemental lines was common, which in some cases were resolved by multipeak fitting allowing an upper limit to still be determined. The crystal structures of the four pRMNs were determined using selected area diffraction (SAD) and microdiffraction patterns, wherein each pRMN was tilted to multiple low-index zones and the patterns were recorded. The d-spacings and angles in the patterns as well as the intrazonal angles were checked for consistency with the known hexagonal metal structures. The (100) and (110) graphite rings present in the SAD patterns were used as an internal distance calibration (approximately 1% accuracy). Further details on the TEM methods employed are available in Croat et al. (2005).

Due to deterioration of the TEM grid substrate, it was not possible to carry out NanoSIMS isotopic measurements of one of the two MUR pRMN-containing sections. Despite lacking isotopic data from this pRMN-containing graphite, it is almost certainly a presolar grain. This is due to the remarkable effectiveness of the physical-chemical separation process and the distinctive appearance of presolar graphites with an onion morphology. After the density-size

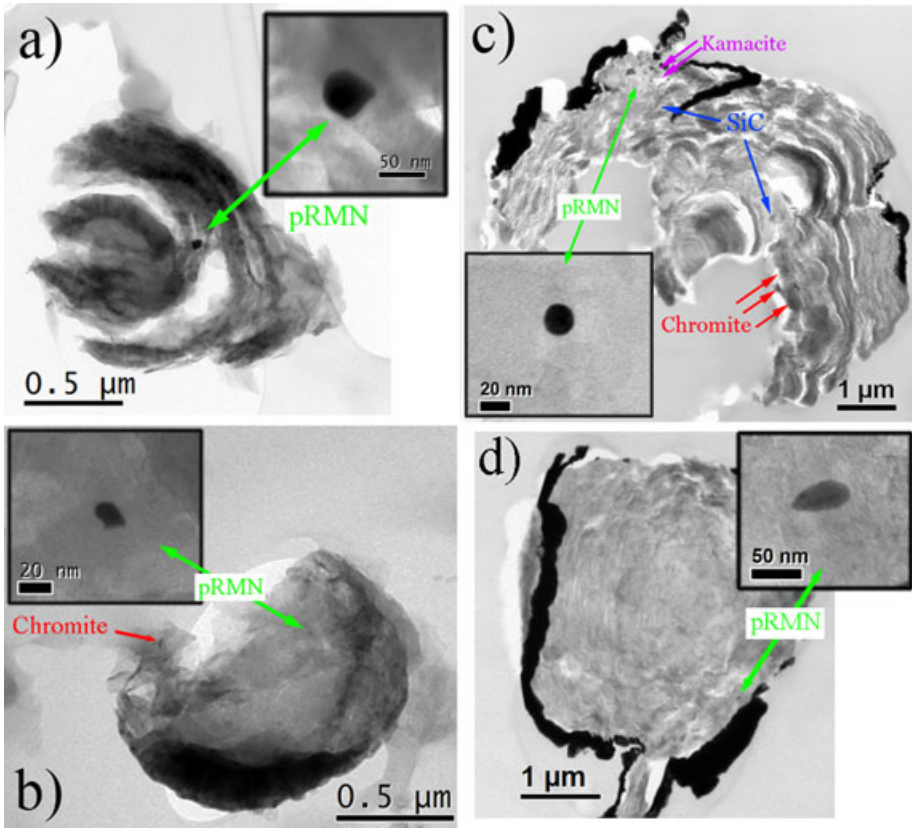

Fig. 1. Bright-field TEM images of pRMNs and their host graphites: a) MUR1 pRMN embedded in graphitized rim region of high-density MUR graphite. b) smaller MUR2 pRMN in nanocrystalline central region of rim-core onion graphite (which also contains chromite grain at periphery). c) ORG1 pRMN (inset close-up) and its host low-density graphite, with symbols indicating positions of the pRMN as well as grains of other phases. The erosion of the graphite section is presumably due to NanoSIMS sputtering and the black regions at the graphite perimeter consist of gold redeposited during prior SIMS analyses. d) ORG2 pRMN at edge of its host graphite again with redeposited gold at perimeter.

separation, approximately 15% of the residue is presolar graphite, with the remainder consisting mainly of larger blocky Si-rich amorphous grains. Thus, after the separation process the graphites are approximately five orders of magnitude more concentrated than they were in the bulk Murchison matrix (with approximately 1 ppm graphite abundance). Furthermore, of approximately 120 unique KFC1 grains measured in the NanoSIMS that had the appearance of onion graphites in TEM, all but three showed C isotopic anomalies that exceeded the 2σ level (Stadermann et al. 2004). The C isotopic distributions of presolar graphite suggest that even those three that lack resolvable C anomalies are probably still presolar grains, but from ancient parent stars that happened to have near solar $^{12}C/^{13}C$ ratios.

RESULTS

Figure 1 shows TEM images of the four pRMNs (referred to hereafter as MUR1, MUR2, ORG1, and ORG2) as well as the graphites in which they are found. In two cases, internal grains of other phases are also found, the ramifications of which are discussed below. The pRMN grain diameters are 53, 16, 21, and 47 nm for MUR1, MUR2, ORG1, and ORG2, respectively, and are found within presolar graphite sections with diameters 1.5, 1.1, 6.9, and 5.0 μm. All pRMNs were identified as hexagonal structures with lattice parameter in the ranges of a = 2.72–2.78 Å and c = 4.30–4.35 Å, in good agreement with literature values for metal compounds with similar compositions (e.g., Os-Ru with a = 2.72, c = 4.30 and Os-Mo with a = 2.76, c = 4.41; Villars and Calvert 1985). Four to six major zones (including the [10-10], [0001], [-12-11], and [2-1-10] zones) were collected during tilting and rotation of TEM studies for each pRMN, and d-spacings, interplanar angles, and intrazonal angles were all consistent with the hexagonal structure. Figure 2 shows an indexed set of four hexagonal TEM microdiffraction patterns collected from different zone axes of the ORG1 pRMN. Table 1 lists the major crystallographic zone axes identified in TEM from each pRMN along with the lattice parameter

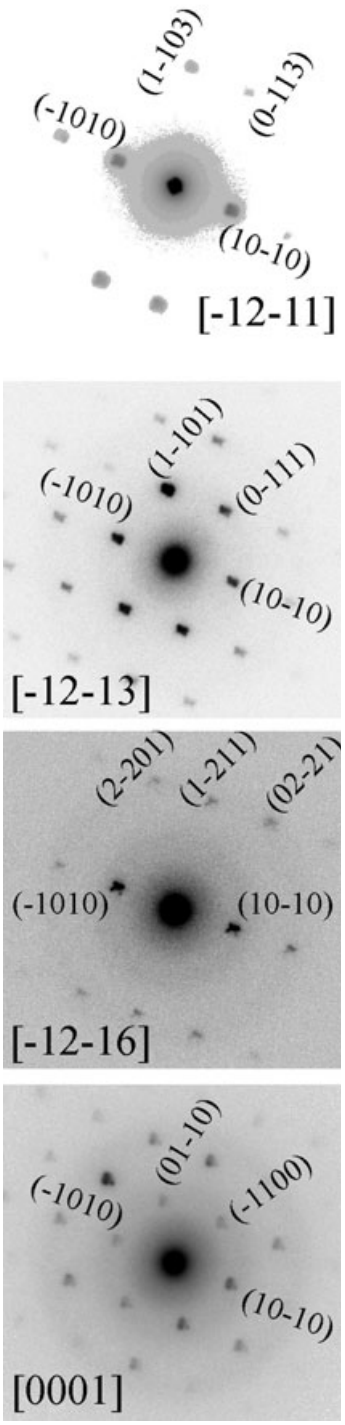

Fig. 2. TEM microdiffraction patterns from four major zone axes of the ORG1 pRMN found while tilting along the (10-10) plane. The spacings and angles between spots in each pattern are consistent with the hexagonal phase (a = 2.75 Å, c = 4.32 Å). In addition, the tilt angles between the zones (calculated from the x,y TEM goniometer readings) are 17.7°, 15.0°, and 30.5°, which agree well with the 17.7°, 14.8°, and 29.9° angles expected between the pairs of zones in the hexagonal structure ([0001] to [-12-16], [-12-16] to [-12-13], and [-12-13] to [-12-11], respectively).

Table 1. Major hexagonal zones indexed for each pRMN with calculated hexagonal lattice parameters.

pRMN	Zones indexed	a	c
MUR1	[100], [210], [31-1], [30-1], [20-1]	2.77 ± 0.06	4.48 ± 0.09
MUR2	[210], [421]	2.74 ± 0.14	4.4 ± 0.2
ORG1	[012], [011], [001], [031]	2.80 ± 0.06	4.44 ± 0.09
ORG2	[-210], [-121], [011]	2.55 ± 0.13	4.6 ± 0.2

determinations for the hexagonal phase. All diffraction patterns revealed single phase structures with no signs of partitioning into compositionally distinct phases (e.g., Mo-rich BCC and OsRuFe-rich hexagonal as suggested by Sylvester et al. 1990). The ORG1 pRMN is anhedral and appeared rounded at all high-symmetry crystallographic zones (Fig. 1c). In contrast, the other three pRMNs from Figure 1 are subhedral, showing some crystal faces characteristic of the hexagonal phase, e.g., MUR1 pRMN is imaged at the [2-1-10] orientation (Fig. 1a), and shows faceting along the (0001) and (01-10) crystal planes.

pRMN Host Graphite and Location

The host graphites of MUR1 and MUR2 (Figs. 1a and 1b) have "onion" morphologies with a central nanocrystalline graphite region surrounded by better-graphitized outer layers (see Croat et al. [2008] for further morphological details on the rim-core morphology). MUR1 has a smaller central nanocrystalline region with approximately 300 nm diameter and the pRMN is found outside this area in one of the well-graphitized onion layers, whereas in MUR2 the pRMN is found in a larger central nanocrystalline region (approximately 700 nm diameter). In both cases, the grain diameters are significantly smaller than the graphite section thickness, so the pRMNs are clearly embedded within the graphite, reducing the possibility that the RMN is a contaminant not native to the presolar graphite. Furthermore, any RMNs that were not embedded within the graphites would typically be found within a higher density fraction of the separate (e.g., approximately 6 g cm^{-3} instead of approximately 2 g cm^{-3}). The ORG1 and ORG2 pRMNs are found at the edges of turbostratic low-density graphite cross sections (Figs. 1c and 1d), and in each case the displayed pRMN is the only one found among multiple cross sections from their host graphite. Although strong (002) diffraction peaks from the stacking of graphene sheets are seen in this type of disordered graphite, these are less well-graphitized than the MUR high-density graphites and also contain significantly higher concentrations of O

Table 2. Elemental concentration of pRMNs found within graphite (in atom%).

pRMN	Os	Ru	Mo	Fe	Ir	W	Pt	Ni	Cr
MUR1	74	9	4	3	2	6	<0.8[a]	<0.8[a]	2
MUR2	37	31	5	5	2	7	<1.1[1]	<1.2[a]	13
ORG1	13	29	24	17	13	1	<0.2[a]	2	1
ORG2	8	18	19	28	7	1	15	4	<0.4[a]

[a]Element is not detected and an upper limit derived from given grain's spectrum is listed.

and other minor elements. As is common among the Orgueil separates, the ORG1 graphite has amorphous, carbonaceous, isotopically solar material adhered to its surface, but the pRMN is found just inside this region and is thus believed to be native to the presolar graphite. The ORG2 pRMN is also found at the graphite's periphery but again is clearly an internal grain.

Table 2 summarizes the EDXS chemical composition of all four pRMNs found within graphite, including all elements detected in any of the grains. Many of the same refractory noble elements that were found in other mRMNs (Wark and Lovering 1976; Eisenhour and Buseck 1992; Berg et al. 2009) are present, although Re and Rh are absent; their low cosmic abundances would prevent their detection in these small grains even if they were greatly enriched over the CI abundances. No significant concentrations of the elements in question are present in EDXS of the graphite or grid background spectra (aside from minor amounts of Fe and Cr). The implications of the observed pRMN compositions are dealt with at length in the Discussion section.

Internal grains of various other phases are found associated with the pRMNs inside the same graphites, including SiC grains in both the ORG1 and ORG2 low-density graphites. Three SiC grains were found within the 16 sections of the ORG1 graphite, one in close proximity to the pRMN and the others near the periphery of different graphite cross sections. The SiCs ranged from 30 to 70 nm in diameter, comparable in size to the pRMNs. They were identified as SiC using electron diffraction, all revealing face-centered cubic structures with a 4.3–4.5 Å lattice parameter. Two of the SiCs were twinned showing the $\Sigma = 3$ twin structure, whereas the other one showed a 1D disordered diffraction pattern and dense stacking faults, both similar to types of presolar SiCs reported by Daulton et al. (2003). One 75 nm SiC was found within the ORG2 graphite, which was identified as the 3C-SiC phase (4.4 Å FCC) based on [011] and [001] FCC diffraction patterns. EDXS showed Si and C along with 2–5 atom% Al and no appreciable Mg that could indicate the presence of decayed ^{26}Al (with Mg/Al upper limits of 0.04–0.07). Two TiCs with diameters of 72 and 24 nm were found in the ORG2 graphite, resulting in a TiC abundance of approximately 30 ppm. No TiCs were found in ORG1 with upper limits of approximately 25 ppm, which is unusual given the ubiquity of TiCs in SN graphites (wherein a single graphite will often contain hundreds of internal TiCs; Croat et al. 2003). However, TiC abundance within graphites is lower among the ^{13}C-rich isotopic subgroup (of which ORG1 is a member). TiCs were also absent from the MUR1 and MUR2 graphites, although in these cases only single graphite cross sections were available. Chromite grains were found in the single section of MUR2 as well as in multiple sections of the ORG1 graphite. Chromite is a known trace phase from the MUR matrix (Fuchs et al. 1973) and since this phase survives the harsh acid etching, like presolar graphites, it is found in higher concentrations in the MUR and ORG grain residues. Often chromite and other Cr-bearing oxides (such as eskolaite) are found adhered to the surface of graphite sections after ultramicrotomy or in some cases appear to overlay the graphites. More rarely, the Cr-bearing grains appear to be internal to the graphite itself. Prior NanoSIMS isotopic measurements of internal chromite grains have shown solar ^{16}O/^{18}O ratios, although only the most extreme anomalies would be detectable in <100 nm chromites such as these. Eight chromite grains from ORG1 appear to be internal grains (far from the periphery) as does the chromite in MUR2, increasing the odds that the chromites are intrinsic to the graphite itself. Furthermore, numerous internal Cr-oxides (eskolaite) were found previously in multiple slices from a KFC1 high-density graphite that also contained metallic RuFe (hexagonal phase) and *s*-process enriched carbides (Croat et al. 2008). It is currently unclear whether the Cr-bearing internal grains are primary condensates or if they instead form by another mechanism, such as oxidation of an existing iron grain by the dichromate solution used during the chemical separation process. Continued isotopic and TEM investigations are thus warranted on these Cr-oxide grains to clarify their origins.

NanoSIMS isotopic measurements, which are available from three of the four RMN-containing graphites, are summarized in Table 3. These indicate that ORG1 is a member of the ^{13}C-rich isotopic subgroup (OR1d3m-7 from Jadhav et al. Forthcoming), which comprises approximately 16% of the low-density and approximately 13% of the high-density graphite populations in ORG (Jadhav et al. Forthcoming) and similar fractions in MUR (Hoppe et al. 1995). The ORG1 graphite and the 29 other low-density OR1d graphites from this mount showed signs of isotopic dilution of minor elements such as N and O relative to other OR1d

Table 3. Isotopic ratios from pRMN-containing graphites.

Sample	$^{12}C/^{13}C$	$^{14}N/^{15}N$	$^{16}O/^{18}O$	$\delta^{29}Si/^{28}Si$[c]	$\delta^{30}Si/^{28}Si$
ORG1 bulk graphite[a]	11.1 ± 0.1	250 ± 15	538 ± 10	−33 ± 11	−6 ± 14
ORG2 bulk graphite[a]	66.0 ± 0.4	263 ± 6	170 ± 3	−140 ± 17	−180 ± 21
MUR1 graphite cross section[b]	135 ± 24	n.a.	505 ± 93	n.a.	n.a.
ORG1 graphite cross sections[b]	10.1 ± 0.4	n.a.	n.a.	−27 ± 24	−32 ± 27
Internal SiC within ORG1[b]	13.4 ± 0.5	n.a.	n.a.	−2 ± 40	−35 ± 46

[a]ORG1 and ORG2 bulk graphite isotopic data reproduced from Jadhav et al. (Forthcoming) and Groopman et al. (2012), respectively, with 1σ errors.

[b]NanoSIMS measurement on TEM cross section; reported errors include 2σ counting statistical errors combined with standard deviation from correction factors derived from standards.

[c]By definition, $\delta^{29}Si/^{28}Si = [(^{29}Si/^{28}Si)_{sample})/(^{29}Si/^{28}Si)_{solar} - 1] \times 1000$.

n.a. = not analyzed.

graphites and relative to those from MUR. Due to the general absence of Si anomalies from all graphites on the mount containing this grain, we suspect a sample contamination issue specific to this mount alone (Jadhav et al. 2008; Jadhav et al. Forthcoming). Thus, the magnitude of the reported minor element anomalies is likely reduced from their true values. For this reason, isotopic measurements made of less abundant species (Ca, Ti, Al-Mg) are reported in Jadhav et al. (Forthcoming) but are not discussed further here. C and Si isotopic measurements were then made on two ORG1 graphite TEM cross sections one of which contained an approximately 70 nm SiC, both to determine if isotopic differences exist between the SiC and graphite as well as to remeasure the Si isotopes in the graphite interior. An isotopic measurement made on a graphite cross section minimizes any possible effect from surface contamination. Table 3 shows that the newly derived Si isotopic ratios from both graphite cross sections and the internal SiC in one of the sections are roughly in agreement with prior bulk measurements by Jadhav et al. (Forthcoming). The C ratio derived from the cross sections is slightly more anomalous than the bulk, possibly reflecting the impact of a small amount of C surface contamination on the bulk measurement. The region containing the internal SiC was slightly less ^{13}C-rich than the surrounding graphite. The ^{13}C enrichment in the SiC was 2.5 times smaller than the standard deviation of $^{12}C/^{13}C$ values from ten randomly selected, similarly sized, grain-free regions within the graphite, suggesting that the difference observed between the SiC and graphite is significant. Isotopic data on the ORG2 graphite (reproduced from Groopman et al. 2012) show large ^{18}O, ^{28}Si and inferred ^{44}Ti enrichments indicative of a SN origin. NanoSIMS imaging mode measurements of ORG2 showed hotspots with correlated ^{18}O and ^{15}N enrichments that likely are associated with the internal TiCs.

NanoSIMS measurements of MUR1 show a clear ^{12}C enrichment but a lack of minor element anomalies; results of this type are common among HD graphites and may be due to isotopic dilution/exchange of minor element anomalies.

DISCUSSION

pRMNs as Primary Condensates Direct from the Gas

Based on the properties of the included pRMNs, we conclude that these grains are direct condensates from the gas. They are single phase crystals rather than complex assemblages and show chemical compositions consistent with chemical fractionation during condensation from the gas. Their single phase microstructure suggests that they are unlikely to have formed via aggregation of smaller grains. As noted in the introduction, formation via later exsolution from graphite is not feasible due to low trace element abundances in graphite, especially for high-density graphites (Zinner et al. 1995). For example, even if the graphite were able to trap enough Os to have a solar Os/C ratio, there would only be enough Os atoms in the entire MUR1 graphite to form an approximately 17 nm Os-rich pRMN by exsolution (not the 50 nm grain observed). pRMN formation separate from and preceding graphite formation is also consistent with the observation of other refractory phases included in graphites, such as carbides (Croat et al. 2003). In many cases, heterogeneous nucleation and growth of iron on existing TiCs prior to encapsulation in graphite and other properties of the internal carbides (e.g., diverse chemical compositions and diverse surface weathering) also demonstrate that these refractory grains are primary condensates from the gas.

Chemical Similarity of pRMNs with mRMNs and Implications for Graphite Condensation

Despite their distinct presolar origin, the pRMNs within graphite follow the chemical trends observed in mRMNs found in CAIs and meteorite matrix, although

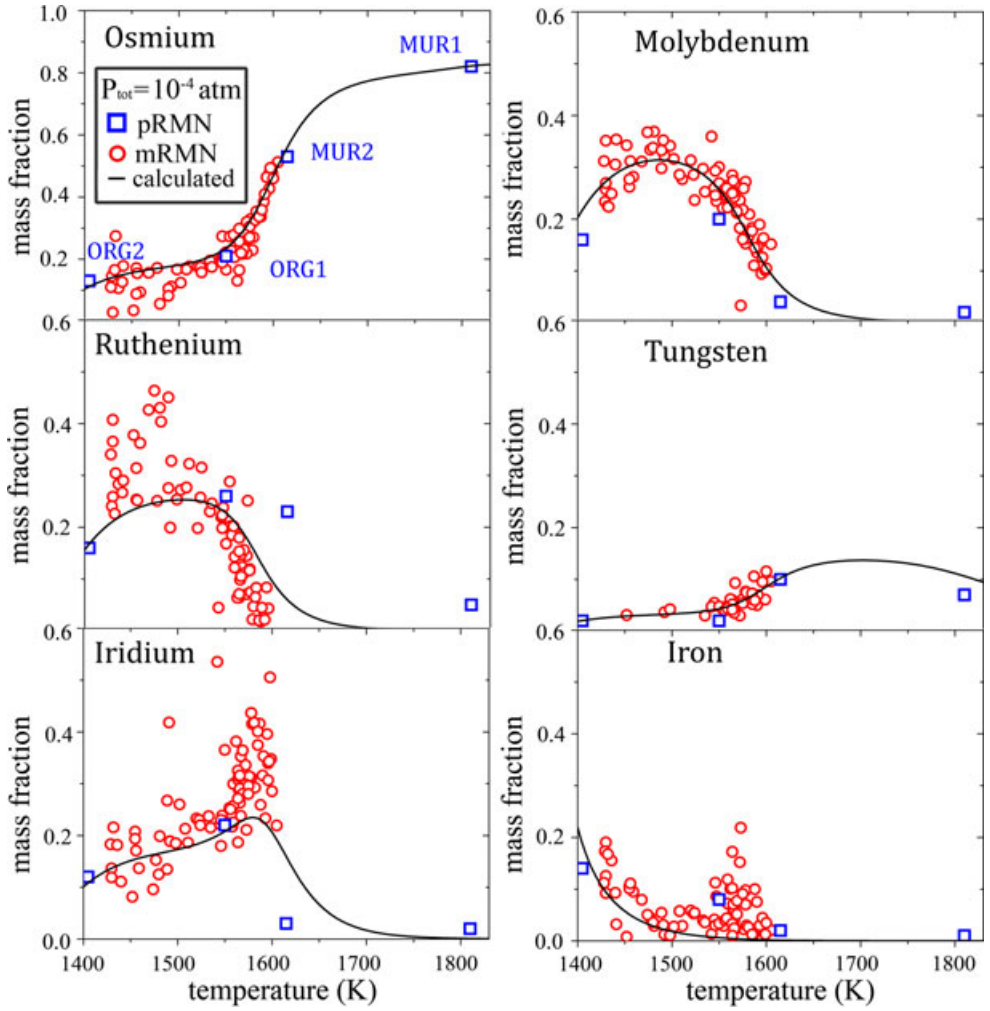

Fig. 3. Elemental composition of presolar RMNs (blue) along with the isolated mRMNs of Berg et al. (2009) (red) plotted as a function of the temperature of last equilibration with the gas, which is calculated using a least squares deviation from the theoretical predictions (solid black line). The solid lines result from equilibrium calculations of RMN compositions as a function of temperature condensing from a solar composition gas (e.g., Palme and Wlotzka 1976).

one of the pRMNs is considerably more refractory. ORG and ORG2 are quite similar to the mRMNs in major elements abundances, showing enrichments of 6.1–6.6 orders of magnitude above CI. These also have comparable minor element abundances of Fe, W, and in some cases Ir. The MUR2 enrichments are more variable, with 5.5–7.0 orders of magnitude above CI, and still within the range seen in mRMNs. The MUR 1 grain, however, is considerably more Os-rich than all of the mRMNs. The compositional variations among the mRMNs cannot be explained by any chemical variations in the gas from which they condensed, but rather by chemical fractionation from a gas of solar composition wherein the mRMNs fall out of equilibrium over a range of temperatures. Figure 3 shows all RMN elemental compositions plotted versus a temperature of last equilibration (adapted from Berg et al. 2009), which is a best fit value derived by matching each grain's composition for multiple elements with predicted values. The most refractory mRMN reported from Berg et al. (2009) was isolated from the gas at 1616K, near the predicted condensation temperature of perovskite. Thus, it was hypothesized that the mRMN compositional range reflects trapping of the mRMN population by various condensing silicate and oxide phases. If one assumes a solar composition and 100 dyne cm^{-2} pressure, the temperatures of last equilibration calculated for MUR1, MUR2, ORG1, and ORG2 are 1810, 1615, 1550, and 1405 K, respectively. The more refractory Os-rich MUR1 pRMN may simply reflect a higher condensation temperature for the high-density graphite in which it was entrained. Furthermore,

the pRMN compositions suggest a lower condensation temperature for the low-density ORG graphites than either of the pRMN-containing high-density graphites. The temperatures of last equilibration inferred from the pRMNs are reasonably consistent with expected graphite condensation temperatures from an otherwise solar composition gas with variable C/O ratio. Lodders and Fegley (1995) calculated graphite condensation temperatures over a pressure range of 10–1000 dyne cm^{-2} (which includes the 100 dyne cm^{-2} pressure of our model), but unlike our model considered higher than solar C/O ratios (1.05 < C/O ratio <10). Fortunately, metal condensation temperatures (for both Fe and W) do not depend on the C/O ratio (e.g., tables 2 and 4c of Lodders and Fegley [1995]; fig. 3 of Lodders and Fegley [1997]). So although the calculated RMN temperatures listed above are pressure-dependent, so too are those of graphite, and thus the sets of temperatures can be directly compared. At C/O = 1.05, graphite condensation is predicted to occur at 1550–1600 K (with a slight dependence on gas pressure; Lodders and Fegley 1995) which is consistent with the 1550 K inferred from the pRMN in the ORG1 graphite. The ORG2 pRMN inferred temperature (approximately 1405 K) falls below this range, possibly indicating formation at C/O values closer to unity, wherein the graphite condensation temperature drops steeply (Lodders and Fegley 1997). As the C/O ratio increases, the condensation temperature ranges also rise, with C/O = 1.2 yielding a 1715–1765 K range and C/O = 2 yielding 1870–1970 K, and thus these higher temperatures are consistent with the MUR1 calculated temperature of 1810 K. As will be discussed, there is also complementary evidence suggesting that low-density graphites do in fact form in the presence of more O than the HD ones. The pRMNs' association with graphite suggests a reducing environment, and perhaps the same is true for the chemically similar isolated mRMNs. Due to the significant elemental fractionation apparent in Fig. 3, it will be more difficult to constrain well the initial composition of the gas from which pRMNs condense, since any significant deviations from the solar ratios (e.g., in Os/Mo) will be masked by the fractionation.

pRMN Implications for mRMNs

The existence of presolar RMNs with elemental compositions comparable to the mRMNs again raises the possibility that some of the mRMN population may be of presolar origin (Wark and Lovering 1976). If present, pRMNs would likely be more abundant among smaller grains due to size limitations on pRMN stardust from kinetic considerations (discussed below). As mentioned in the introduction, isotopic measurements on mRMNs that would clarify their origins are quite limited to date. Isotopic ratios (e.g., of Os, Ru, and Mo) in pRMNs would likely show deviations from solar, but measurement of such anomalies in small pRMNs presents considerable experimental difficulties. Only very large isotopic anomalies would be resolvable in the small pRMNs using current SIMS techniques such as NanoSIMS. A new generation of resonant-ionization mass spectrometers (e.g., Stephan et al. 2010) may increase the ion yield enough to allow definitive isotopic measurements of smaller RMNs. For the LD graphites (ORG1 and ORG2) the pRMNs are at the graphite's periphery raising the possibility that they are not native to the graphite. The pRMN diameters are considerably less than the graphite section thickness, diminishing the odds that they were dragged from the surface during ultramicrotomy. Furthermore, the phase associations in the LD ORG graphites, namely that less refractory pRMNs are found along with less refractory (and uncommon) SiC grains and with few or no TiCs, strengthens the case that these pRMNs are native to the ORG presolar graphites. The argument that pRMNs are native to the HD graphites is even stronger, in that the grains are clearly embedded near the graphite's center and again smaller than the ultramicrotome slice thickness. Also, more refractory Os-rich pRMNs (such as MUR1) are not found among the hundreds of reported mRMNs (Berg et al. 2009), so a nonnative origin is not feasible.

Stellar Source(s) of pRMN-Containing Graphites

The ORG2 pRMN-containing graphite is unambiguously of SN origin based on its observed enrichments in ^{18}O, ^{28}Si, and ^{44}Ti (Groopman et al. 2012). The isotopic data from the ORG1 graphite, which show a large ^{13}C enrichment but lack significant minor element anomalies, are less diagnostic since such C isotopic anomalies can originate in various stellar environments. Other insights into the origins of the ^{13}C-rich graphite subgroup, which comprises approximately 20% of the low-density graphite population in Murchison and Orgueil, come from TEM studies. Like ORG1, four of the six other low-density ^{13}C-rich graphites studied do not contain TiCs (with upper limits on TiC abundances of 60–150 ppm), and the remaining two have relatively low TiC abundances of 23 and 265 ppm (Croat et al. 2012). In contrast, TiCs are ubiquitous in other LD SN graphites (those with clear ^{18}O and ^{28}Si excesses), with TiC abundances relative to graphite of several thousand ppm and with many individual graphites containing hundreds of internal TiCs (Croat et al. 2003, 2010b, 2011). The ^{13}C-rich LD

graphites do often contain kamacites and embedded internal chromites and in cases SiCs and amorphous silicate grains (g9 from Croat et al. 2010b). The internal TiCs found in the two ^{13}C-rich LD graphites lacked the *s*-process element enrichments seen in AGB graphites, and instead were chemically similar to those in SN graphites. Furthermore, NanoSIMS isotopic measurement of one such TiC showed an ^{18}O enrichment that greatly exceeded that of its host ^{13}C-rich graphite, and which indicated a SN origin for the assemblage (with the graphite likely experiencing a higher degree of isotopic exchange or dilution). It should be noted though that the NanoSIMS Ti count rates from ORG1 were sufficiently high to suggest the presence of a Ti-rich phase, but one sputtered away during the SIMS measurement (Jadhav et al. Forthcoming). Taken together, while the ^{13}C-rich graphites such as ORG1 shows appreciable differences from the LD SN graphites with clearly diagnostic ^{18}O and ^{28}Si isotopic anomalies (differences which are consistent with a lower graphite condensation temperature for ^{13}C-rich graphites based on inclusions found), there are clear indications of a SN origin for members of this group. Determining whether the two pRMN-containing HD graphites also originate in SNe is complicated by a lack of isotopic data (clear C anomaly in MUR2 but no data from MUR1). The HD and LD graphite populations do have a different distribution of stellar sources, with SN signatures more common in LD graphites (Jadhav et al. Forthcoming) and AGB signatures more common in HD graphites (e.g., Croat et al. 2005; Zinner et al. 2006). Isotopic evidence from many HD graphites, namely large ^{12}C enrichments accompanied by large ^{30}Si and smaller ^{29}Si enrichments, are consistent with a low-metallicity AGB origin for many members of this group (Zinner et al. 2006). However, among the HD graphites there are also counter-examples showing isotopic evidence of formation in massive stars, such as the HD MUR graphites with unusual SiCs (Croat et al. 2010a) or HD ORG graphites with evidence of decayed ^{44}Ti (Jadhav et al. Forthcoming). Thus, while they are clearly presolar at present we can only narrow the stellar source of pRMNs to any environment that lacks large relative abundance variations of the metals found in RMNs.

Relationship between Stellar Source and Graphite Density, Morphology, and Isotopic Properties

Any explanation of the differences observed between the pRMN-containing LD graphites (ORG1 and ORG2) and the HD ones (MUR1, MUR2) should take into account the interrelationships between graphite density, morphology, and other properties, such as their minor element content (especially O). Distinct presolar graphite morphologies were evident in early SEM-based studies, which classified the graphites as "onions" or "cauliflowers" based on their surface appearance (Hoppe et al. 1995). SIMS measurements of these graphites showed that the more disordered low-density structures such as cauliflowers had considerably higher O and other minor element content. Subsequent TEM-based studies further clarified the graphite structures and demonstrated a correlation between the graphite morphology and the stellar source and other grain properties (Croat et al. 2008). Experimental TEM studies of carbonaceous materials (often formed by pyrolysis) show microstructural variations similar to those observed in presolar graphites (Oberlin 1989). In these studies, the introduction of heteroatoms such as O and S in the carbonaceous materials disrupts the normal process of graphitization, resulting in more turbostratic disorder (Oberlin 1989). This is likely caused by cross-linking of adjacent graphene sheets by O bonded at the edges of the sheets, preventing sheets from rearranging into more perfect graphite. The occurrence of this mechanism in graphite forming from environments with lower C/O ratios is a likely cause of both the greater disorder and higher O content in "cauliflower" graphites. It is also possible that LD graphites could become disordered for other reasons (e.g., forming more rapidly at higher supersaturation) and then have higher O content simply because their structures have more available O sites. However, the ORG1 and ORG2 graphites also have pRMN compositions that suggest a lower graphite condensation temperature, and this lower temperature could be a result of lower C/O ratios in the gas from which the graphite condensed. Taken together, the observed differences between the HD and LD pRMN-containing graphites form a self-consistent picture. When the LD graphites form in regions with lower C/O ratios, the higher O content causes graphite disorder, lower density, and higher O content captured by the grain, and the graphite's concomitant lower condensation temperature causes its included pRMNs to show less refractory compositions. For the HD graphites, condensation in more C-rich environments allows graphite to form at higher temperatures and capture RMNs that are more refractory, and also to have lower included O content which then allows rearrangement into a denser, more ordered structure. The cross-linking of O into the LD graphite's structure may also explain their better retention of O isotopic anomalies in comparison with HD graphites, which tend to show evidence for isotopic anomaly dilution of any isotopes that are not retained within their internal carbides.

Grain Growth Kinetics of pRMNs

Since the pRMNs have been established as direct condensates from the gas, the observed grain sizes and compositions can give some insight into temperatures and pressures of the environment from which they condensed. A key question is whether these pRMNs can reasonably grow to the observed size from gas with nearly solar relative abundances of metals or if instead they require chemically peculiar stellar environments. The compositional similarities between the four pRMNs and mRMNs forming in the solar system suggest that any compositional differences in the gas are not extreme. Regarding the grain sizes, a useful point of comparison for pRMNs is with other presolar grain types from both SN and AGB environments, such as presolar TiCs in graphite. For example, presolar TiC median sizes are 24 nm (observed size range of 7–81) for AGB carbides and 90 nm (range: 15–480) for SN carbides. Detailed modeling of the growth of presolar TiCs and graphite has been done for AGB outflows (Bernatowicz et al. 2005) and similar considerations can also be applied to the grain growth in SN (as seen in Croat et al. 2003). The simplest grain growth model ignores the difficult question of nucleation and biases results in favor of growth by considering that it is only limited by the arrival of the rate-limiting species on the surface of a growing grain. Such simplifying assumptions (e.g., near unity sticking coefficient) are supported by recent experimental studies of metal condensation (Tachibana et al. 2011). If one assumes a similar temperature range for growth (e.g., 1800 to 1000 K for both TiC and pRMNs), then the model predicts that the ratio of the maximum grain diameters to which each phase can grow is related to the abundance of the rate-limiting species in the gas. This type of comparison of maximum presolar grain diameters has been successfully applied to TiC and graphite growth in AGB outflows (Bernatowicz et al. 2005). Such a model predicts that the maximum graphite diameter should be approximately 200× larger than the maximum TiC diameter (3.8 μm graphite and 18 nm TiC, respectively, in Bernatowicz et al. 2005), whereas the observed ratio of maximum sizes is approximately 50× (4 μm graphite and 75 nm TiC, respectively; Croat et al. 2008). The discrepancy may be partially explained by various complicating factors that are specific to the TiC–graphite size comparison; one must use not the C gas number density itself but the amount of free carbon above that locked into CO, and also an adjustment should be made for the expected longer growth interval for TiC (see Bernatowicz et al. 2005). Applying the same logic to the growth of the largest Os-rich pRMN (MUR1) in an AGB outflow, with an Os/Ti abundance ratio of 2.8×10^{-4} in a solar gas, the same conditions that lead to observed approximately 75 nm TiCs in AGB graphites (e.g., Bernatowicz et al. 2005) would result in an approximately 4.8 nm Os-rich pRMN, which is an order of magnitude smaller than the observed MUR1 pRMN. However, the growth model does suggest a few parameters that could increase the pRMN diameter, namely higher overall gas pressure or higher Os relative abundance (both of which increases the Os gas number density) or perhaps a longer interval over which pRMNs can grow. Thus, we now consider various possible formation environments and the degree to which each could grow larger pRMNs.

The first possibility is formation in a SN outflow rather than an AGB star, and again we can use presolar TiC sizes as a basis for comparison. In fact, isotopic evidence indicates such an origin for the ORG1 and ORG2 pRMNs in LD graphite, so a SN origin is also conceivable for the MUR1 pRMN (despite the evidence that many HD graphites have a low-metallicity AGB origin; Zinner et al. 2006). SN presolar grains are typically larger than AGB ones but are quite variable; certain graphites have median TiC sizes comparable to AGB carbides but others contain significantly larger TiCs (up to approximately 500 nm which represents an approximately 10× increase over the largest AGB carbide). This suggests that there is no more than an order of magnitude difference between SN and AGB grain forming environments in terms of typical gas pressures or grain formation intervals. Like AGB stars, various lines of evidence point to grain growth intervals of several years (e.g., Moseley et al. 1989; Hoppe and Besmehn 2002). The observed condensation sequences are also similar (TiC then graphite), which suggests that the overall pressures do not differ greatly. With Os as the rate-limiting species and using the solar Os/Ti ratio, the same growth conditions leading to a maximum TiC diameter of approximately 500 nm would result in an approximately 60 nm pRMN at the ORG2 compositions, which compares favorably to the observed grain diameter of 47 nm. If the MUR1 pRMN were also of SN origin, an approximately 31 nm maximum diameter would be predicted for such an Os-rich pRMN, considerably closer to its observed diameter of 53 nm.

Consideration of Low-Metallicity AGB Environments

Although an SN origin is plausible for the pRMNs in HD graphite, the high ^{12}C enrichments along with $^{29,30}Si$ enrichments often seen in HD graphites are consistent with a low-metallicity AGB origin (Zinner et al. 2006). As such, the effects of a lower metallicity

on pRMN growth should be considered. Recent stellar surveys have revealed significant numbers of metal-poor stars (both in the galactic halo and in the LMC and SMC), and detailed astronomical observations of such stars (e.g., carbon enhanced metal-poor [CEMP] stars) can be a useful guide to pertinent nucleosynthetic trends in lower-metallicity stars (e.g., Beers and Christlieb [2005] and references therein). In addition, stellar models developed in concordance with these stellar observations (e.g., Bisterzo et al. 2011) provide further insight. Some of these observed objects (e.g., CEMP s with *s*-process enrichments in the galactic halo) are of sufficiently low mass that they could not have evolved quickly enough to contribute dust to the solar nebula (e.g., Bernatowicz et al. 2005). However, it is believed that their observed *s*-process enrichments result from higher mass AGB binary companions that do evolve more quickly, and thus the compositional trends observed may yet be relevant for the low-metallicity carbon-rich AGB stars that produced presolar grains. Furthermore, IR spectral studies of dust around low-metallicity stars show that the lower-metallicity C stars can still produce carbonaceous dust (Sloan et al. 2006). Some of these metal-poor stars show significant carbon enrichments (e.g., CEMP giant stars; Suda et al. 2011) and thus would be more conducive to the formation of carbonaceous stardust. One might assume that a pRMN (a metal grain) would be less likely to condense in a metal-poor star, but this is not necessarily true. The metal-poor moniker is defined based on iron observations (e.g., $[Fe/H] < -2$ where $[Fe/H] = \log_{10}(Fe/H)_{star} - \log_{10}(Fe/H)_{solar}$), but some of the stars with large C enrichments can have nearly solar overall metal content (defined in the astronomical sense as $Z > 2$). Furthermore, large excesses in n-capture elements are common in CEMP stars, often showing abundance enrichments of several orders of magnitude (e.g., $[Ba/Fe] > 2$). A subset of these metal-poor stars shows *r*-process enrichments, with Os enrichments of 30–50× with respect to solar Os/Fe ratios (Beers and Christlieb 2005). The combined Os and Ru content of the MUR1 pRMN is approximately 85 atom%, and both of these elements are *r*-process dominated (with approximately 90% of solar Os and approximately 70% of solar Ru coming from the *r*-process). Thus, an *r*-process enriched and C-rich source of the type observed among lower-metallicity CEMP-r stars is an attractive origin. This also makes the prospect of isotopic measurements of internal pRMNs more interesting, and such measurements may be possible with the increased ion yield and spatial resolution of resonant-ionization mass spectrometers currently under development (Stephan et al. 2010). These results suggest that Os abundances in low-metallicity AGB stars can be enriched by perhaps an order of magnitude, similar to the maximum enrichments expected from SN environments discussed above. These considerations suggest that a low-metallicity AGB origin is also possible for the pRMNs found inside HD graphites.

CONCLUSIONS

We report the results from TEM investigations of four refractory metal nuggets found within presolar graphites, both from the high-density MUR fraction and the low-density ORG size-density fractions. Although we do not have isotopic information on the pRMNs themselves, these 30–50 nm grains are clearly embedded within presolar graphites. Their formation via exsolution is not plausible, which points to their formation as direct condensates from the gas in a circumstellar environment (either AGB or SN outflows). The pRMNs are compositionally diverse (e.g., from 8 to 74 atom% Os), but the observed compositions fall on the same trend lines defined by mRMNs found in meteorites (Berg et al. 2009), suggesting chemical fractionation dependent upon the temperature of last equilibration with the gas. The temperatures of last equilibration range from 1405 to 1810 K are in good agreement with the predicted temperature range for graphite condensation (Lodders and Fegley 1995) at plausible C/O ratios. One of the pRMNs is significantly more refractory (Os-rich) than all mRMNs (Berg et al. 2009), reflecting the higher condensation temperature of graphite relative to melilite, spinel, and other phases that encapsulate mRMNs. Based on the composition of internal pRMNs, which are isolated from the gas once entrained in graphite, the high-density graphites form at higher temperatures than the low-density ones. This can be explained if the high-density graphites condense from gas with higher C/O ratios, wherein the graphite formation temperature is elevated (Lodders and Fegley 1995). A relatively more O-rich condensation environment leaves other imprints on the low-density graphites, namely their higher O-minor element concentrations (Zinner et al. 1995). Moreover, the O itself likely impedes the graphitization process leading to increased turbostratic disorder and lower density (Oberlin 1989). Like the other isolated mRMNs found within meteorites, the pRMNs within graphite are single-phase hexagonal crystals; this along with the chemical similarity supports the conclusions of Berg et al. (2009) that the mRMNs are also direct condensates from the gas (but ones that condense in the early solar system rather than being presolar). However, the discovery of presolar RMNs also raises the possibility that some of the smaller mRMNs may also be presolar, and further isotopic measurements on these grains are warranted.

Although their small size prevents detection of any isotopic anomalies in the pRMNs themselves, we have isotopic data from three of four of their host graphites which confirm a presolar origin. Isotopic measurements of one pRMN-containing LD graphite show large ^{18}O, ^{28}Si, and inferred ^{44}Ti enrichments, which clearly indicate a SN origin. The other LD graphite only shows a ^{13}C enrichment and lacks diagnostic minor element anomalies, preventing definitive identification of its stellar source. However, it contains internal SiCs that are normally associated with SN graphites, and other members of this group (namely ^{13}C-rich LD graphites with low TiC abundances) have shown evidence of a SN origin. Other than a clear ^{12}C enrichment in one pRMN-containing HD graphite, we lack the isotopic data required to determine their stellar source. However, other KFC1 HD graphites predominantly show isotopic evidence for a low-metallicity AGB origin (Zinner et al. 2006), and like refractory TiCs, the pRMNs may form in multiple types of carbonaceous-grain environments. One useful method to confirm that pRMNs can reasonably grow in SN or low-metallicity AGB environments is to compare their grain diameters with those of other typical presolar phases such as TiC and graphite. Using a simple model wherein growth is limited only by the number density of the rate-limiting species, the grain diameters of the two pRMNs within LD graphite are reasonable when compared with TiCs known to grow in SN outflows. The most Os-rich pRMN in HD graphite exceeds its expected size by an order of magnitude based on the sizes of AGB TiCs also found in HD graphite. However, the size of this pRMN can plausibly be increased to match its observed size through higher Os gas number densities that could be present either in low-metallicity AGB stars or in SNe.

Acknowledgments—We thank Teruyuki Maruoka for preparation of the Orgueil graphite separate and Emily Lebsack (Washington University) for preparation of TEM sections from the ORG1 graphite. This material is based on work supported by NASA grant NNX10AI45G issued through the Office of Space Science.

Editorial Handling—Dr. Ian Lyon

REFERENCES

Amari S., Lewis R. S., and Anders E. 1994. Interstellar grains in meteorites: I. Isolation of SiC, graphite, and diamond; size distributions of SiC and graphite. *Geochimica et Cosmochimica Acta* 58:459–470.

Beers T. C. and Christlieb N. 2005. The discovery and analysis of very metal-pool stars in the galaxy. *Annual Review of Astronomy and Astrophysics* 43:531–580.

Berg T., Marosits E., Maul J., Schanhense G., Hoppe P., Ott U., and Palme H. 2009. Direct evidence for condensation in the early solar system and implications for nebular cooling rates. *The Astrophysical Journal* 702:L172–176.

Bernatowicz T. J., Cowsik R., Gibbons P. C., Lodders K., Fegley B., Jr., Amari S., and Lewis R. S. 1996. Constraints on stellar grain formation from presolar graphite in the Murchison meteorite. *The Astrophysical Journal* 472:760–782.

Bernatowicz T. J., Akande O. W., Croat T. K., and Cowsik R. 2005. Constraints on grain formation around carbon stars from laboratory studies of presolar graphite. *The Astrophysical Journal* 631:988–1000.

Bernatowicz T. J., Croat T. K., and Daulton T. L. 2006. Origin and evolution of carbonaceous presolar grains in stellar environments. In *Meteorites and the early solar system II*, edited by Lauretta D. S. and McSween H. Y., Jr. Tucson, Arizona: The University of Arizona Press. pp. 109–126.

Bisterzo S., Gallino R., Straniero O., Cristallo S., and Käppeler F. 2011. The *s*-process in low-metallicity stars—II. Interpretation of high-resolution spectroscopic observations with asymptotic giant branch models. *Monthly Notices of the Royal Astronomical Society* 418: 284–319.

Blum J. D., Wasserburg G. J., Hutcheon I. D., Beckett J. R., and Stolper E. M. 1988. "Domestic" origin of opaque assemblages in refractory inclusions in meteorites. *Nature* 331:405–409.

Croat T. K., Bernatowicz T., Amari S., Messenger S., and Stadermann F. J. 2003. Structural, chemical, and isotopic microanalytical investigations of graphite from supernovae. *Geochimica et Cosmochimica Acta* 67:4705–4725.

Croat T. K., Stadermann F. J., and Bernatowicz T. J. 2005. Presolar graphite from AGB stars: Microstructure and *s*-process enrichment. *The Astrophysical Journal* 631:976–987.

Croat T. K., Stadermann F., and Bernatowicz T. 2008. Correlated isotopic and microstructural studies of turbostratic presolar graphites from the Murchison meteorite. *Meteoritics & Planetary Science* 43:1497–1516.

Croat T. K., Stadermann F., and Bernatowicz T. 2010a. Unusual $^{29,30}Si$-rich SiCs of massive star origin found within graphites from the Murchison meteorite. *The Astrophysical Journal* 139:2159–2169.

Croat T. K., Jadhav M., Lebsack E., and Bernatowicz T. J. 2010b. Microstructural differences in TEM among the isotopic groups of low-density Orgueil graphites (abstract #1585). 41st Lunar and Planetary Science Conference. CD-ROM.

Croat T. K., Jadhav M., Lebsack E., and Bernatowicz T. J. 2011. A unique supernova graphite: Contemporaneous condensation of all things carbonaceous (abstract #1533). 42nd Lunar and Planetary Science Conference. CD-ROM.

Croat T. K., Groopman E., Amari S., and Bernatowicz T. J. 2012. TEM insights into the stellar origins of the ^{13}C-rich graphite subgroup. *Meteoritics & Planetary Science* 47: A5242.

Daulton T. L., Bernatowicz T. J., Lewis R. S., Messenger S., Stadermann F. J., and Amari S. 2003. Polytype distribution of circumstellar silicon carbide:

Microstructural characterization by transmission electron microscopy. *Geochimica et Cosmochimica Acta* 67:4743–4767.

Eisenhour D. D. and Buseck P. R. 1992. Transmission electron microscopy of RMNs: Implications for single-phase condensation of the refractory siderophile elements. *Meteoritics* 27:217.

El Goresy A., Nagel K., and Ramdohr P. 1978. Fremdlinge and their noble relatives. Proceedings, 9th Lunar and Planetary Science Conference. pp. 1279–1303.

Fuchs L., Olsen E., and Jensen K. J. 1973. Minerology, mineral chemistry and composition of the Murchison (C2) meteorite. *Smithsonian Contributions to the Earth Sciences* 10:1–39.

Groopman E., Bernatowicz T. J., and Zinner E. 2012. C, N and O isotopic heterogeneities in low-density supernova graphite grains from Orgueil. *The Astrophysical Journal* 754:L8.

Grossman L. 1980. Refractory inclusions in the Allende meteorite. *Annual Review of Earth and Planetary Science* 8:559–608.

Hoppe P. and Besmehn A. 2002. Evidence for extinct vanadium-49 in presolar silicon carbide grains from supernovae. *The Astrophysical Journal* 576:L69–72.

Hoppe P., Amari S., Zinner E., and Lewis R. S. 1995. Isotopic compositions of C, N, O, Mg, and Si, trace element abundances, and morphologies of single circumstellar graphite grains in four density fractions from the Murchison meteorite. *Geochimica et Cosmochimica Acta* 59:4029–4056.

Hutcheon I. D., Armstrong J. T., and Wasserburg G. J. 1987. Isotopic studies of Mg, Fe, Mo, Ru and W in Fremdlinge from Allende refractory inclusions. *Geochimica et Cosmochimica Acta* 51:3175–3192.

Jadhav M., Amari S., Zinner E., and Maruoka T. 2006. Isotopic analysis of presolar graphite grains from Orgueil. *New Astronomy Reviews* 50:591–595.

Jadhav M., Amari S., Marhas K. K., Zinner E., Maruoka T., and Gallino R. 2008. New stellar sources for high-density presolar graphite grains. *The Astrophysical Journal* 682:1479–1485.

Jadhav M., Amari S., Zinner E., Maruoka T., Marhas K.K., and Gallino R. Forthcoming. Multi-element isotopic analyses of presolar graphite grains from Orgueil. *The Astrophysical Journal*.

Lodders K. and Fegley B., Jr. 1995. The origin of circumstellar silicon carbide grains found in meteorites. *Meteoritics* 30:661–678.

Lodders K. and Fegley B., Jr. 1997. Condensation chemistry of carbon stars. In *Astrophysical implications of the laboratory study of presolar materials*, edited by Bernatowicz T. J. and Zinner E. New York: American Institute of Physics. pp. 391–424.

MacPherson G. J., Wark D. A., and Armstrong J. T. 1988. Primitive material surviving in chondrites: Refractory inclusions. In *Meteorites and the early solar system*, edited by Kerridge J. F. and Matthews M. S. Tucson, Arizona: The University of Arizona Press. pp. 746–807.

Moseley S. H., Dwek E., Glaccum W., Graham J. R., Loewenstein R. F., and Silverberg R. F. 1989. Far-infrared observations of thermal dust emission from supernova 1987A. *Nature* 340:697–699.

Oberlin A. 1989. High-resolution TEM studies of carbonization and graphitization. In *Chemistry and physics of carbon*, edited by Thrower P., vol. 22. New York: Dekker. pp. 1–143.

Palme H. and Wlotzka F. 1976. A metal particle from a Ca, Al-rich inclusion from the meteorite Allende, and the condensation of refractory siderophile elements. *Earth and Planetary Science Letters* 33:45–60.

Sloan G. C., Kraemer K. E., Matsuura M., Wood P. R., Price S. D., and Egan M. P. 2006. Mid-infrared spectroscopy of carbon stars in the Small Magellanic Cloud. *The Astrophysical Journal* 645:1118–1130.

Stadermann F. J., Croat T. K., and Bernatowicz T. 2004. NanoSIMS determination of carbon and oxygen isotopic compositions of presolar graphites from the Murchison meteorite (abstract #1758). 35th Lunar and Planetary Science Conference. CD-ROM.

Stadermann F. J., Croat T. K., Bernatowicz T. J., Amari S., Messenger S., Walker R. M., and Zinner E. 2005. Supernova graphite in the NanoSIMS: Carbon, oxygen and titanium isotopic compositions of a spherule and its TiC sub-components. *Geochimica et Cosmochimica Acta* 69:177–188.

Stephan T., Davis A. M., Pellin M. J., Savina M. R., and Veryovkin I. V. 2010. CHILI—The Chicago instrument for laser ionization—A progress report (abstract #2321). 41st Lunar and Planetary Science Conference. CD-ROM.

Suda T., Yamada S., Katsuta Y., Komiya Y., Ishizuka C., Aoki W., and Fujimoto M. Y. 2011. The Stellar Abundances for Galactic Archaeology (SAGA) data base — II. Implications for mixing and nucleosynthesis in extremely metal-poor stars and chemical enrichment of the galaxy. *Monthly Notices of the Royal Astronomical Society* 412: 843–874.

Sylvester P. J., Ward B. J., Grossman L., and Hutcheon I. D. 1990. Chemical compositions of siderophile element-rich opaque assemblages in an Allende inclusion. *Geochimica et Cosmochimica Acta* 54:3491–3508.

Tachibana S., Nagahara H., Ozawa K., Ikeda Y., Nomura R., Tatsumi K., and Joh Y. 2011. Kinetic condensation and evaporation of metallic iron and implications of metallic iron dust formation. *The Astrophysical Journal* 736: 1–8.

Villars P. and Calvert L. D. 1985. *Pearson's handbook of crystallographic data for intermetallic phases*, vol. 3. Metals Park, OH: American Society of Metals.

Wark D. A. and Lovering J. F. 1976. Refractory/platinum metal grains in Allende calcium-aluminium-rich clasts (CARC's): Possible exotic presolar material? 7th Lunar and Planetary Science Conference. pp. 912–914.

Zinner E., Amari S., Wopenka B., and Lewis R. S. 1995. Interstellar graphite in meteorites: Isotopic compositions and structural properties of single graphite grains from Murchison. *Meteoritics* 30:209–226.

Zinner E., Amari S., and Jadhav M. 2006. On the stellar sources of presolar graphite. In *Proceedings of the international symposium "Nuclei in the cosmos—IX."* CERN, Geneva, June 25–30, 2006. Proceedings of Science, PoS (NIC-IX) 019.